belmadan@hawaii.edu

Wind-induced baroclinic beta-plumes and the Hawaiian Lee Counter-Current

Ali Belmadani [1], Nikolai Maximenko [1], Oleg Melnichenko [1], Niklas Schneider [1,2], and Emanuele Di Lorenzo [3]
(1) IPRC/SOEST/UH, Honolulu, HI (2) Oceanography Department/SOEST/UH, Honolulu, HI (3) SEAS/GATech, Atlanta, GA

Introduction

A planetary **β-plume** is a classical example of oceanic circulation induced by a **localized vorticity source** or sink that allows an analytical description in simplistic cases. Its barotropic structure is a zonally-elongated, gyre-like cell governed by the **Sverdrup** circulation on the β-plane. The dominant zonal currents, found west of the source/sink, are often referred to as **zonal jets**.

This simple picture describes the depth-integrated flow. Many previous studies have investigated β-plumes in a reduced-gravity framework or using other simple models with a small number of vertical layers, thereby lacking representation of the **vertical structure**. In addition, most previous studies consider a purely linear regime without considering the role of **eddies**. However, these jets are often associated with strong lateral shear that makes them unstable under increased forcing. The circulation in such a nonlinear regime may involve eddy-mean flow interactions, which modify the time-averaged circulation.

Here, the **baroclinic** structures of **linear** and **nonlinear wind-forced β-plumes** are studied using a **continuously-stratified**, **eddy-permitting ocean model**. Implications for the **Hawaiian Lee Counter-Current** – a real-world example of β-plume – are discussed.

Conclusion

To our knowledge, this is the first description of the **vertical structure of a nonlinear β-plume** induced by localized vorticity forcing. In the **linear case**, a **westward decay of the surface jets** occurs simultaneously with a **deepening of the plume**, while a **zonally-uniform barotropic flow** forms west of the forcing region, in agreement with **Sverdrup dynamics**. In the **nonlinear case**, mesoscale **eddies dissipate the surface jets and zonal transport**. However, this only takes place in the forcing region: to the west, the barotropic flow is zonally uniform.

The westward change in vertical structure is found to be partly due to **baroclinic Rossby wave damping by vertical viscosity**, which suppresses higher-order modes more efficiently, leading to a westward increase in the relative contribution of lower-order modes. The **shape of the β-plume** is partly determined by the **spatial scale of the forcing** that influences the **vertical propagation of Rossby waves**: shallower (deeper) with an extended (reduced) forcing area.

This is also the first time that a **deep extension** is found **below the Hawaiian Lee Counter-Current**. High-resolution eddy-resolving simulations show **baroclinic and barotropic structures consistent with the idealized model** experiments, and similar sensitivity to the scale of the wind stress curl in the lee of Hawaii. Some ***in-situ* observations** also support these results. The possible effect of bottom topography in dissipating zonal transport is now being studied.

Linear β-Plume: Analytical vs. Numerical Solutions

Wind stress: (fig. 1a,b)

$$\tau_x = \frac{\tau_{max}\sqrt{e}}{R} y.e^{-\frac{x^2+y^2}{2R^2}}, \quad R = 40\ km$$

$$\tau_y = -\frac{\tau_{max}\sqrt{e}}{R} x.e^{-\frac{x^2+y^2}{2R^2}}$$

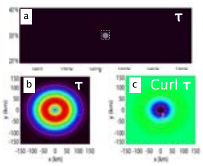

Fig 1 (a),(b) **Surface wind stress**. *(c)* **Wind stress curl**. Negative is for downwelling.

Ekman pumping is derived from wind stress curl (fig. 1c). The **Sverdrup** relation on the **β-plane** is then used to compute meridional transport, which is localized in the forcing region.

Zonal transport is finally derived from the **continuity equation** and from **geostrophy**.

Zonal Transport: (fig. 2a)

$$U = \frac{\tau_{max}\sqrt{e}}{\rho R^4 \beta} y.e^{-\frac{y^2}{2R^2}} \left\{ \sqrt{\frac{\pi}{2}}\left(3R^2 - y^2\right)\left[erf\left(\frac{x_e}{\sqrt{2}R}\right) - erf\left(\frac{x}{\sqrt{2}R}\right)\right] - R\left[x.e^{-\frac{x^2}{2R^2}} - x_e.e^{-\frac{x_e^2}{2R^2}}\right]\right\}$$

$x_e \approx 2890\ km$
$\rho = 1025\ kg.L^{-1}$
$\beta \approx 1.98\ 10^{-11}\ s^{-1}m^{-1}$

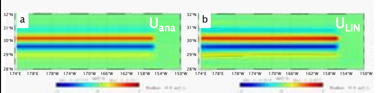

Fig 2 **Zonal transport**: *(a)* analytical and *(b)* numerical (LIN) solutions.

The **ROMS** solution (fig. 2b) under **weak forcing** (LIN) is in very **good agreement with a theoretical linear β-plume** (fig. 2a). The zonal transport is slightly overestimated by ~25%.

The linear regime exhibits an **anticyclonic cell** (2 jets) at ~30°N flanked by **2 weaker cyclonic cells**. All 4 **jets are purely zonal** and extend all the way to the western boundary.

Linear vs. Nonlinear β-Plumes: Snapshots vs. Time-Mean Circulation

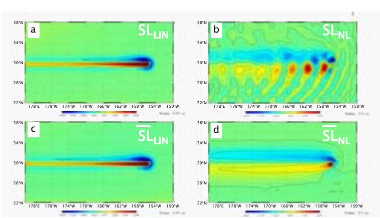

Fig 3 **Sea level snapshots** after 20 model years in *(a)* LIN and *(b)* NL, **mean sea level** in *(c)* LIN and *(d)* NL.

In **LIN**, **snapshots** (fig. 3a) **mimic the steady-state circulation** (fig. 3c), which is established via Rossby wave propagation.

In **NL**, **eddies** are shed in the forcing region (fig. 3b) and then propagate westward. The complex structure of instantaneous sea level suggests an interplay between eddies and Rossby waves. Eddies also **rectify the mean circulation**, from tripolar in LIN (fig. 3c) to bipolar in NL (fig. 3d).

Linear β-Plume: Baroclinic Structure

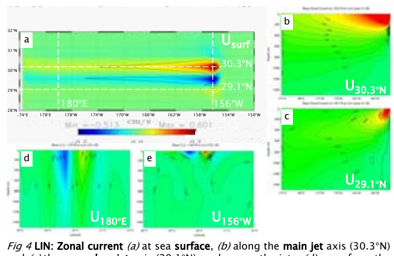

Fig 4 **LIN**: **Zonal current** *(a)* at sea **surface**, *(b)* along the **main jet** axis (30.3°N) and *(c)* the **secondary jet** axis (29.1°N), and across the jets, *(d)* **away** from the forcing region (180°E), and *(e)* in the **forcing region** (156°W).

A fast **westward decay of the surface jets** (fig. 4a) appears in striking contrast with the barotropic flow (fig. 2b). This is associated with a **deepening** of the lower boundary of the strong anticyclonic **plume** (fig. 4b), and a deepening of the core of the weaker cyclonic plume (fig. 4c).

Vertical sections across the jets confirm that **deep currents appear away from the forcing region** (fig. 4d,e) and compensate the surface decay in terms of transport (fig. 2b). Westward jets are a mirror image of eastward jets.

Nonlinear β-Plume: Baroclinic Structure

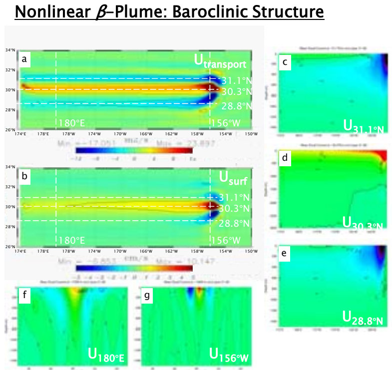

Fig 5 **NL**: *(a)* **Zonal transport** and **current** *(b)* at sea **surface**, *(c)* along 31.1°N, *(d)* 30.3°N and *(e)* 28.8°N, and across the jets, *(f)* **away** from the forcing region (180°E), and *(g)* in the **forcing region** (156°W).

Eddies dissipate zonal transport in the forcing region, resulting in a broader circulation pattern (fig. 5a). However, **transport is zonally uniform a few degrees to the west** of the forcing region.

A **westward decay of the surface jets** is evident both in the forcing region and west of it (fig. 5b). For the **eastward flowing jet**, **a deepening** of the flow is seen in the deeper layers (fig. 5d). A **deepening** of the core of the secondary **westward flowing jets** is also evident (fig. 5c,e).

Vertical sections across the jets reveal that the meridional broadening of the surface flow is compensated by the formation of **subsurface counter-currents** away from the forcing region (fig. 5f,g).

Vertical Viscosity and Baroclinic Rossby waves

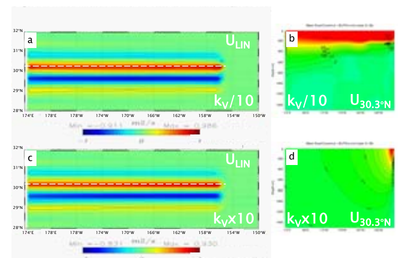

Fig 6 Same as (Fig.2b, Fig.4b) but with vertical viscosity *(a,b)* 10 times weaker ($k_V=10^{-4}m^2s^{-1}$) and *(c,d)* 10 times stronger ($k_V=10^{-2}m^2s^{-1}$).

The baroclinic structure changes over a smaller (larger) zonal scale when vertical viscosity is increased (reduced), while the barotropic flow is unchanged: this suggests a possible **baroclinic Rossby wave damping by vertical viscosity**, which suppresses higher-order modes more efficiently.

In linear and nonlinear cases, **doubling the forcing spatial scale** (and max. wind so that max. curl is unchanged) induces a **shallower plume with weaker westward change** (fig. 7b,d). This suggests **vertically-propagating Rossby waves** may be involved. Zonal transport becomes more linear (fig. 7a,c), possibly because of weaker meridional shear / barotropic instability.

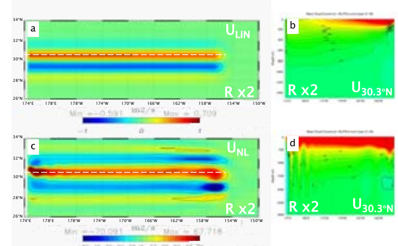

Fig 7 *(a,b,c,d)* same as (Fig.2b, Fig.4b, Fig.5a, Fig.5d) but with wind vortex radius twice longer (R=80 km). Color scale in (c) is different than in Fig.5a.

Implications for the Hawaiian Lee Counter-Current

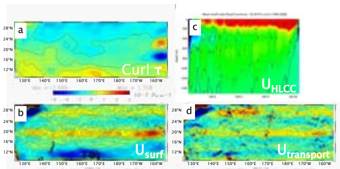

Fig 8 **HLCC in OFES-N**: mean *(a)* **wind stress curl**, **zonal current** *(b)* at sea **surface** and (c) **along the jet** axis, and *(d)* **zonal transport**. Currents were highpass-filtered to remove the large-scale gyre circulation.

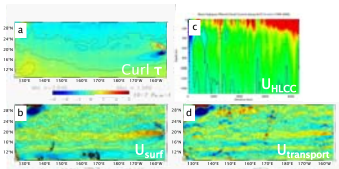

Fig 9 Same as Fig. 8 but for **OFES-Q**.

HLCC is a **β-plume** forced by **wind stress curl** west of Hawaii (Yu et al. 2003). The forcing scale (fig. 8a, 9a) sets the HLCC meridional scale (fig. 8b, 9b, 8d, 9d), as in LIN (fig. 2b, 7a). A **westward decay** is evident, particularly in OFES-Q (fig. 9b).

The HLCC **baroclinic structure** is **similar to LIN** (fig. 4b, 7b) in OFES-N (fig. 8c), but **also to NL** (fig. 5d, 7d). In comparison, the **plume in OFES-Q** (fig. 9c) is more easily compared to ROMS simulations with a **more localized wind** forcing (fig. 4b, 5d), consistently with the narrower QuickSCAT curl (fig. 9a) compared to NCEP (fig. 8a).

Also, the HLCC **transport is zonally-uniform west of Hawaii** in OFES-N (fig. 8d) as in LIN or NL (fig. 2b, 5a), but it is **not as obvious in OFES-Q** (fig. 9d). This may be due to bottom friction since Rossby waves likely have a stronger vertical component in OFES-Q.

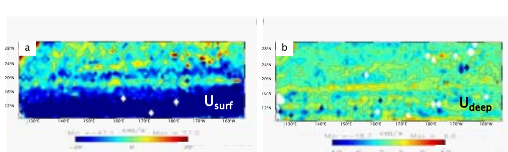

Fig 10 **Mean zonal current** *(a)* at sea **surface** and *(b)* at **depth** from **YoMaHa**'07 data.

YoMaHa velocities further suggest the baroclinic β-plume framework may be relevant for the HLCC: while **maximum surface currents** are found in the **lee of Hawaii** (fig. 10a), they are found **near 140–165°E at deeper levels** (fig. 10b).

Models and Data

ROMS model

The **ROMS** (Shchepetkin and McWilliams 2005) is a free surface, hydrostatic model that resolves the primitive equations using stretched sigma-coordinates. It is configured for an **idealized subtropical ocean** (20°N to 40°N, 60° in longitude) with a **flat bottom** (4000m). A **1/3°** resolution allows eddies to form, and **10 vertical levels** resolve the baroclinic circulation.

The model is forced at the surface by a **steady anticyclonic Gaussian wind vortex**, which provides a localized vorticity source in the center of the domain (fig. 1a,b). The associated **wind stress curl and Ekman pumping** comprise **downwelling** in the vortex center, surrounded by a **ring of weaker upwelling** (fig. 1c).

A spatially-uniform initial stratification typical of the North Pacific subtropical gyre is derived from the World Ocean Atlas 2009. It is also prescribed at every time step along the open boundaries to **avoid any large-scale currents** induced by horizontal density gradients. Vertical mixing is uniform and steady: $k_T=10^{-7}m^2s^{-1}$, $\mathbf{k_V=10^{-3}m^2s^{-1}}$. The simulation is started from rest and run for **30 years** with 20 min time step (20 s for the barotropic mode). Outputs are saved every 5 days.

2 sets of simulations are analyzed: **LIN** (**weak forcing**: 10^{-3} Nm^{-2} max wind stress) and **NL** (**strong forcing**: 10^{-1} Nm^{-2} max).

OFES model

The **OFES** (Masumoto et al. 2004) is a **global eddy-resolving** ocean model based on the GFDL MOM3 code with **1/10°** resolution and **54 vertical levels**. Monthly means are used here.

2 runs are analyzed over 1999-2008: **OFES-N** (NCEP forcing) and **OFES-Q** (QuickSCAT forcing).

ARGO-YoMaHa data

The **YoMaHa'07** dataset (Lebedev et al. 2007) provides estimates of **surface** and **deep currents** derived from trajectories of 4284 **ARGO** floats over 1997-2007.

Surface velocities are linearly regressed from float coordinates fixed by satellite. Deep velocities are estimated from float displacements during each submerged phase of the cycle.

References

Lebedev, K., H. Yoshinari, N. A. Maximenko, and P. W. Hacker, 2007: YoMaHa'07: Velocity data assessed from trajectories of Argo floats at parking level and at the sea surface. *IPRC Technical Note*, **4** (2), 16p.
Masumoto, Y., et al., 2004: A fifty-year eddy-resolving simulation of the world ocean—Preliminary outcomes of OFES (OGCM for the Earth Simulator). *J. Earth Simulator*, **1**, 35-56.
Shchepetkin, A. F., and J. C. McWilliams, 2005: The Regional Oceanic Modeling System: A split-explicit, free-surface, topography-following-coordinate ocean model. *Ocean Modelling*, **9**, 347-404.
Yu, Z., N. Maximenko, S.-P. Xie, and M. Nonaka, 2003: On the termination of the Hawaiian Lee Countercurrent. *Geophys. Res. Lett.*, **30**(5), 1215, doi:10.1029/2002GL016710.

Acknowledgements

The OFES simulations were conducted on the Earth Simulator (Japan), and access to the outputs was provided by the APDRC of the IPRC. YoMaHa'07 data was also provided by the APDRC. This research was supported by JAMSTEC, NASA, and NOAA through their sponsorship of the IPRC. Additional support was provided by NASA through grant NNX08AR49G.